

Photocatalytic study of Zinc Oxide with bismuth doping prepared by spray pyrolysis

Tzu-Yang Lin¹, Yu-Ting Hsu², Wen-How Lan^{*1}, Chien-Jung Huang³,
Lung-Chien Chen^{**4}, Yu-Hsuan Huang¹, Jia-Ching Lin⁵, Kuo-Jen Chang⁵,
Wen-Jen Lin⁵ and Kai-Feng Huang²

¹Department of Electrical Engineering, National University of Kaohsiung 811, Taiwan

²Department of Electrophysics, National Chiao Tung University, Hsinchu 300, Taiwan

³Department of Applied Physics, National University of Kaohsiung, Kaohsiung 811, Taiwan

⁴Department of Electro-Optical Engineering, National Taipei University of Technology, Taipei 106, Taiwan

⁵Materials and Electro-Optics Research Division, National Chung-Shan Institute of Science and Technology, Taoyuan 325, Taiwan

(Received August 4, 2015, Revised November 30, 2015, Accepted December 1, 2015)

Abstract. The unintentionally doped and bismuth (Bi) doped zinc oxide (ZnO) films were prepared by spray pyrolysis at 450°C with zinc acetate and bismuth nitrate precursor. The n-type conduction with concentration $6.13 \times 10^{16} \text{cm}^{-3}$ can be observed for the unintentionally doped ZnO. With the increasing of bismuth nitrate concentration in precursor, the p-type conduction can be observed. The p-type concentration $4.44 \times 10^{17} \text{cm}^{-3}$ can be achieved for the film with the Bi/Zn atomic ratio 5% in the precursor. The photoluminescence spectroscopy with HeCd laser light source was studied for films with different Bi doping. The photocatalytic activity for the unintentionally doped and Bi-doped ZnO films was studied through the photodegradation of Congo red under UV light illumination. The effects of different Bi contents on photocatalytic activity are studied and discussed. Results show that appropriate Bi doping in ZnO can increase photocatalytic activity.

Keywords: zinc oxide, bismuth doping, photocatalytic, spray pyrolysis

1. Introduction

The photocatalytic technology has received great attention in the past decades. Under the light illumination, the photocatalytic materials (Fujishima and Honda 1972, Wongkalasina *et al.* 2001, Cai *et al.* 2014, Szabo *et al.* 2004) destruct the organic contaminants in water, transform to carbon dioxide and leave no waste. In these photocatalytic materials, the zinc oxide (ZnO) based material, which have been applied in electronic and optoelectronic field (Lin and Yan 2011, Fah and Wang 2000, Wan *et al.* 2010, Lin and Chen 2010), was widely investigated as it is inexpensive, chemically stable and nontoxic properties (Song *et al.* 2011).

*Corresponding author, Professor, E-mail: whlan@nuk.edu.tw

**Corresponding author, Professor, E-mail: ocean@ntut.edu.tw

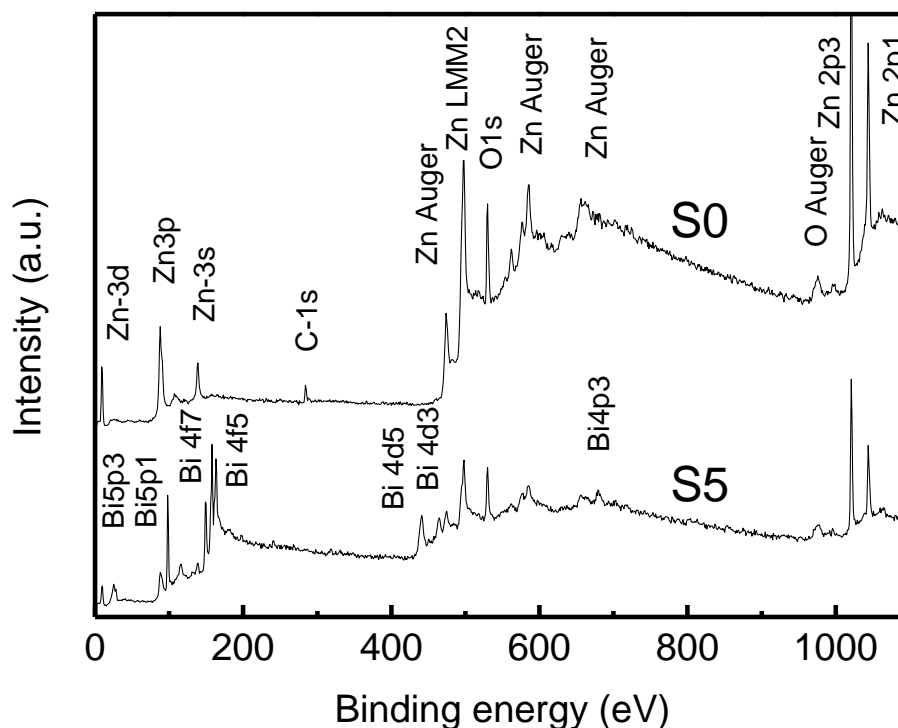


Fig. 1 XPS spectra of survey spectrum for ZnO (S0) and ZnO:Bi (S5).

In order to enhance the photocatalytic efficiency, some efforts have applied (Cao *et al.* 2012, Li *et al.* 2013). Within these methods, the doping technology generally shows effects. In the fabrication of ZnO, various deposition technologies have been developed (Wu *et al.* 2009, Chen *et al.* 2007, Paraguay *et al.* 1999, Islam and Podder 2009). The spray pyrolysis is one of the attractive deposition technique for obtaining large-area film without high vacuum module. In our previous study, we fabricate p-type ZnO from sufficient Bi doping by spray pyrolysis (Huang *et al.* 2014). According to J. B. Zhong's work (Zhong *et al.* 2012) and our study (Hsu *et al.* 2014), Bi doped ZnO shows a talent photocatalytic ability.

In this work, we report the film properties and photodecomposition ability for the ZnO films with different Bi content by spray pyrolysis. The electrical conduction and photoluminescence analysis were applied to characterize the films. The photodecomposition ability of Congo red (CR) under UV light irradiation for the unintentionally doped and Bi-doped ZnO films was studied.

2. Experiment

The unintentionally doped (u-) and bismuth (Bi) doped ZnO was deposited on n-Si substrate at 450°C by spray pyrolysis (Huang *et al.* 2014). With standard RCA cleaning process on Si substrate followed by rinse in buffer oxide etchant cleaning, the wafer was transferred to deposition chamber (Yu *et al.* 2013). An aqueous solution with zinc acetate was used as a precursor. The concentration of the solution was 0.2M. Bismuth doping was achieved by adding bismuth nitrate to the solution.

The atomic ratio of bismuth to zinc (Bi/Zn) was fixed at 0, 1%, 5% and 7% with sample indices S0, S1, S5 and S7 respectively.

The XPS (PHI Quantera SXM) was utilized to study the element composition and bonding. The carrier type, carrier concentration and mobility were obtained by Hall measurement by van der Pauw four-point probe method by Keithley 2611 multimeter with a magnetic field strength of 4.2T at room temperature. The 10K photoluminescence (PL) measurement were carried out by HR2000+ system with a He-Cd (325nm) laser and a cryostat. For photocatalytic study, samples were cut to 2 cm×2 cm size. The degradation of Congo red (CR) was carried out in 100mL CR with concentration 10ppm with sample at room temperature under a 10W low pressure mercury lamp (UV) irradiation. Before the UV irradiation, the solution was stirred in the dark for 10 min for stabilization. The concentration of CR was determined by the transmission of the solution at wavelength 520 nm.

3. Results and discussion

Fig. 1 shows the XPS spectrum for the unintentionally doped ZnO (S0) and Bi doped ZnO (S5) films. For sample S0, except for the surface contaminated carbon signal, the characteristic peaks are associated with zinc and oxygen (Kumar *et al.* 2013, Pradhan *et al.* 2012). For sample S5, peaks contributed from zinc, oxygen and bismuth can be observed. No characteristic peaks of other elements were found. Fig. 2 shows the individual peaks for (a) Bi 4f, (b) O 1s and (c) Zn 2p signals of sample S0 and S5.

Fig. 2(a) shows the Bi 4f_{7/2}(158.6eV) and Bi4f_{5/2} (163.8eV) peaks for sample S5. Signal in this range for S0 was shown also as reference. With the similarly reported value (Lee *et al.* 2011), Bi³⁺ may formed in the film. Fig. 2(b) shows the binding energy of O 1s for the two samples. For sample S0, the two peaks are resolved as 529.4eV and 531.1eV. The peak at 529.4eV represents the O 1s signal in the ZnO. The peak at 531.1eV is attributed to the formation of zinc hydroxide with chemisorbed oxygen species (Gogurla *et al.* 2014). For sample S5, peaks at 529.8 eV and 531.1eV can be observed respectively. The peak position for the chemisorbed oxygen species remains the same. The peak position for O 1s in ZnO is shift to higher energy. Beside, a shoulder of the peak 529.8eV can be observed also. The binding energy peak of O is found to be shifted toward higher values compared to sample S0. With the distorted O 1s and the formation of Bi³⁺, the substitution of O by Bi is expected in the structure. In Fig. 2(c), for the Zn 2p_{3/2} peaks, a slightly broaden signal for S5 compared to S0 can be observed. This broadening may cause from the change of chemical state of Zn with the incorporation of Bi in the structure.

The electrical properties for the unintentionally doped ZnO (S0) and Bi doped ZnO (S1, S5 and S7) are show in Table 1. For sample S0, as nitrogen vacancy and/or zinc interstitial may incorporate during the film formation (Xu *et al.* 2004), n-type conduction can be observed. For sample S1, S5 and S7, p-type conduction can be observed. For ZnO with Bi doping, as the bismuth substitution into the oxygen site may occurred as discussed above and hole (p-type) may dominate the conduction type (Kumar *et al.* 2013). The hole concentration increases with the increasing of Bi content. For sample S5 and S7, the concentration was nearly the same, shows the concentration saturation behaviour. The mobility decreases with the increasing of Bi content. With introduced Bi content in the film, the impurity scattering may shorten the carrier lifetime and thus decrease the mobility. The conductivity, as affected by concentration and mobility, thus shows a relative maximum quantity for sample S5.

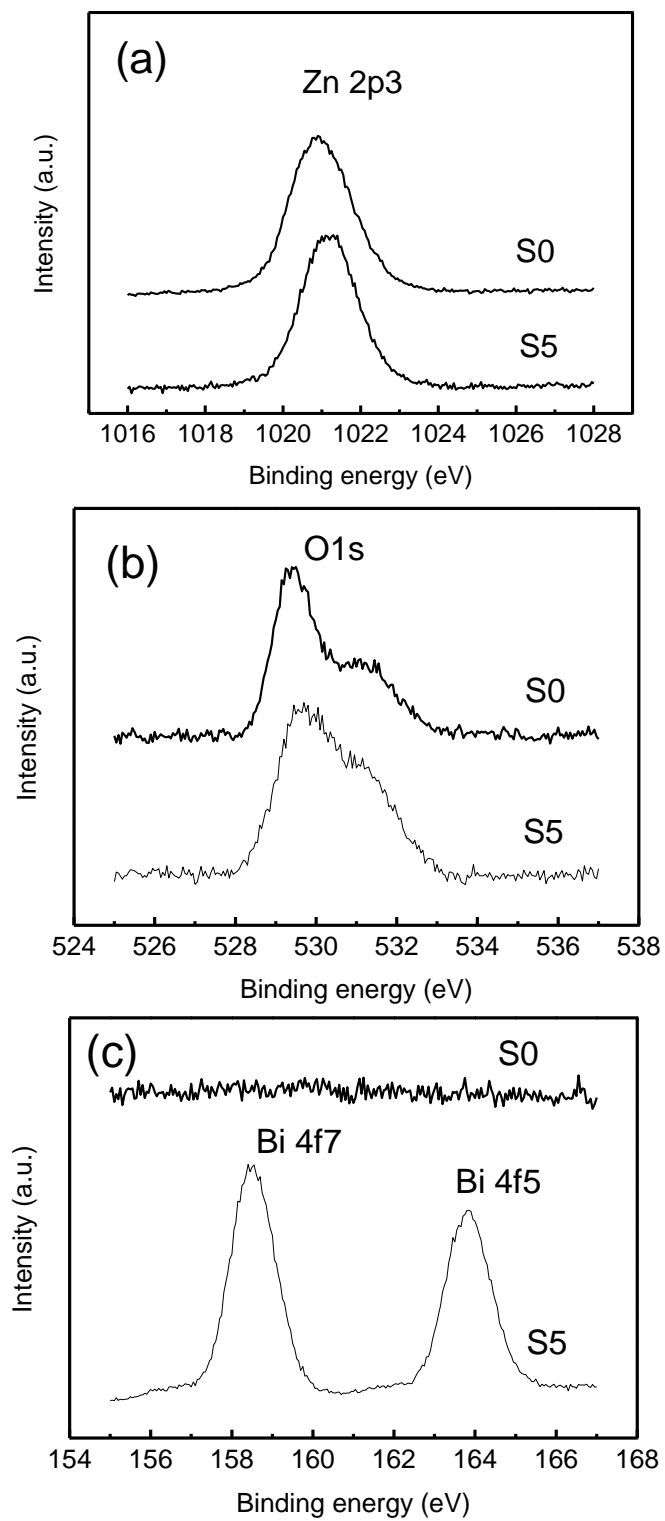


Fig. 2 XPS spectra for ZnO(S0) and ZnO:Bi(S5) of (a) Bi 4f; (b) O 1s; and (c) Zn 2p

Table 1 The electrical properties for ZnO (S0) and ZnO:Bi (S1, S5, S7) samples

Sample	composition	Conduction type	Concentration (cm ⁻³)	Conductivity (S/cm)	Mobility (cm ² V ⁻¹ s ⁻¹)
S0	ZnO	<i>n</i>	6.13×10 ¹⁶	0.13	13.2
S1	ZnO:Bi(1%)	<i>p</i>	2.01×10 ¹⁷	0.21	6.40
S5	ZnO:Bi(5%)	<i>p</i>	4.44×10 ¹⁷	0.39	5.53
S7	ZnO:Bi(7%)	<i>p</i>	4.58×10 ¹⁷	0.33	4.55

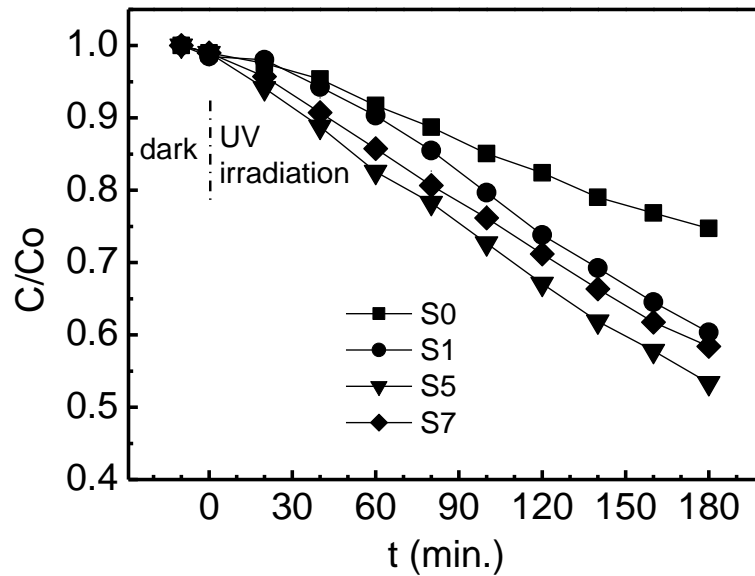
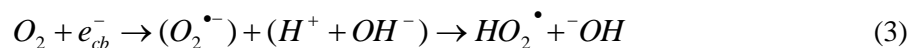
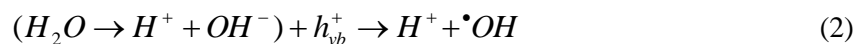


Fig. 3 The photocatalytic activity of samples S0, S1, S5 and S7 in the degradation of CR under UV irradiation

Fig. 3 shows the photocatalytic activity of samples S0, S1, S5 and S7 in the photo degradation of CR under UV irradiation. The C_0 and C are the initial concentration (10 ppm) of CR and the concentration of exposure time t . For the solution remains in dark ($t=-10-0$ min), a negligible concentration variation can be observed. While under UV irradiation, the concentration of CR shows a decreasing behavior with the increasing of exposure time. While after 180min irradiation, the C/C_0 values are 0.75, 0.60, 0.58 and 0.53 for sample S0, S1, S5 and S7, respectively. Sample S5 has the highest photocatalytic ability. For sample S0 to S5, the concentration increases with the increasing of Bi. The reaction of photodecomposition can be expressed as (Chandraboss *et al.* 2013, Senthilvelan *et al.* 2013)





The Eq. (1) shows the electron/hole (e_{cb}^{-} / h_{vb}^{+}) generation due to the absorption of photon with energy $h\nu$ greater than the bandgap. Once the charge separation is maintained, the electron and hole may migrate to the surface of photocatalyst ZnO where they take part in the redox reactions with CR in water in the presence of oxygen. The hole may react with the surface bound H_2O to produce the hydroxyl radicals (${}^{\bullet}OH$) Eq. (2) which attack dye (CR) molecular successively to make degradation. Also, the electron is picked up by oxygen to generate superoxide radical anions ($O_2^{\bullet-}$) Eq. (3). In the meanwhile, hole could interact with HO_2^{\bullet} and ${}^{-}OH$ forming ${}^{\bullet}OH$ radical which attack the dye also. With the successive photocatalytic cycle, radicals decompose the dye into H_2O and CO_2 .

For samples S0 to S5, the hole concentration and the conductivity increases with the increasing of Bi content. With higher conductivity, the electron and hole could migrate to the surface easily and thus cause the higher decomposition ability of CR. Yet for sample S7, although the hole concentration is high, the mobility is less. This suggests hole scattering is more and the move ability of hole is less. With this, the supply of hole to the surface may reduce and limit the radical generation in Eq. (2) and Eq. (4). Thus lower photodecomposition ability can be expected.

To further understanding, low temperature PL analysis was applied. Fig. 4 shows the 10 K PL spectra of the four samples. For sample S0, a near band edge (NBE) emission with peak wavelength 367.6 nm (3.373eV) (Rastogi *et al.* 2004) can be observed. The intensified peak with wavelength 372.0 nm (3.333eV) is attribute to near band edge emission of bounded neutral donors ($D^{\circ}X$) (Zhong *et al.* 2012). The emission wavelength 380.0 nm (3.263eV) and 388.3 nm (3.193eV)

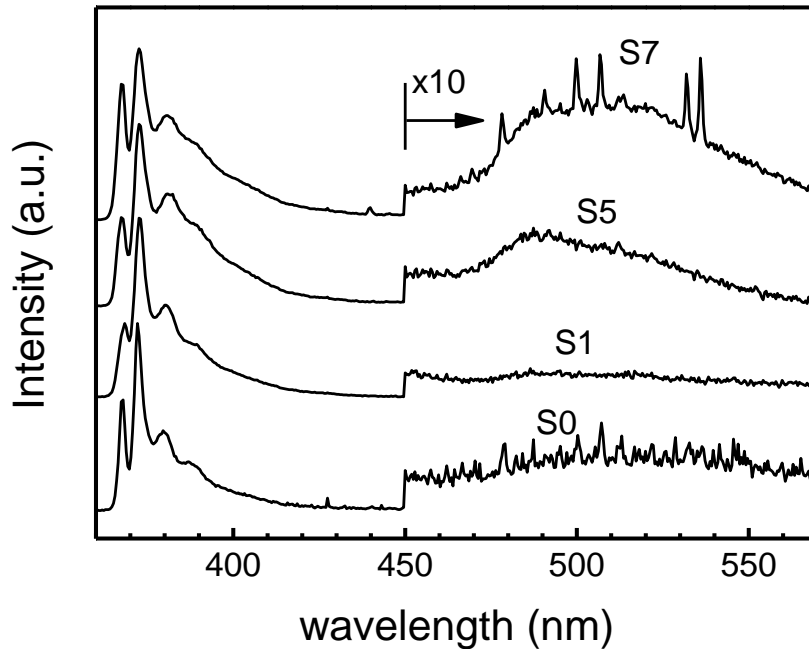


Fig. 4 The 10K photoluminescence spectra of the unintentionally doped ZnO (S0) and ZnO:Bi films with different Bi content(S1, S5 and S7)

is attribute to the phonon replica of $D^{\circ}X$. A broad band around 500 nm (2.48eV) which is known as green-emission (Bhaskar *et al.* 2009) can be observed. This peak is attribute to the singly ionized oxygen vacancy (Golshahi *et al.* 2009, Fan *et al.* 2013) and/or zinc interstitial (Fan *et al.* 2013).

For sample S1, S5 and S7, similar NBE emissions can be observed. The intensified signal is at wavelength 372.6 nm (3.328eV). This peak, with less energy compared to $D^{\circ}X$ which can be observed by other Bi-doped ZnO (Lee *et al.* 2011), is attributed to $A^{\circ}X$ caused by Bi doping. The emission wavelength 381.3 nm (3.252eV) and 390.3 nm (3.177eV) may attribute to the phonon replica of $A^{\circ}X$. Besides, a broaden peak around 490 nm can be observed. As this peak is different with the green-emission for the undoped ZnO (S0) and can only be observed for the Bi-doped ZnO samples. This may attribute to the Bi-related state. For sample S7 with high Bi content, the emission spectrum around 490 nm distorted and become broaden (485 nm-530 nm). Thus a more complex state formed for the high Bi-contented ZnO sample. With these states, carrier scattering becomes stronger and hole and electron may recombine through these states (Chandraboss *et al.* 2013). Both reduce the carrier migration ability to surface. Thus the photodecomposition ability for S7 is reduced.

4. Conclusions

ZnO thin films with Bi-doping were prepared by spray pyrolysis deposition method. With Hall measurement, p-type conduction with concentration around 10^{17} cm^{-3} can be observed. These films were used for the photodegradation of Congo red (CR) under UV-light irradiation. The photodegradation of CR on ZnO and ZnO:Bi films with different Bi content in aqueous solution were studied. Appropriate Bi doping in ZnO can enhance its photocatalytic ability. The 10K photoluminescence analysis has been applied to realize the film quality. The mechanism of photocatalytic ability ZnO films with different Bi content has been discussed.

Acknowledgements

This research is supported by National Science Council, R.O.C. under contract Nos. MOST 104-2221-E-390-011-MY2 and by National Chung Shan Institute of Science and Technology, R.O.C. under contract Nos. CSIST-310-V402(104).

References

- Bhaskar, R., Lakshmanan, A.R., Sundarajan, M., Ravishankar, T., Jose, M.T. and Lakshminarayan, N. (2009), "Mechanism of green luminescence in ZnO", *Ind. J. Pure Appl. Phys.*, **47**, 772-774.
- Cai, X., Cai, Y., Liu, Y., Deng, S., Wang, Y., Wang, Y. and Djerdj, I. (2014), "Photocatalytic degradation properties of Ni(OH)₂ nanosheets/ZnO nanorods composites for azo dyes under visible-light irradiation", *Ceram. Int.*, **40**, 57-65.
- Cao, J., Li, X., Lin, H., Chen, S. and Fu, X. (2012), "In situ preparation of novel p-n junction photocatalyst BiOI/(BiO)₂CO₃ with enhanced visible light photocatalytic activity", *J. Hazard. Mater.*, **239**, 316-324.
- Chandraboss, V.L., Natanapatham, L., Karthikeyan, B., Kamalakkannan, J., Prabha, S., Senthilvelan, S. (2013), "Effect of bismuth doping on the ZnO nanocomposite material and study of its photocatalytic

- activity under UV-light”, *Mater. Res. Bull.*, **48**, 3707-3712.
- Chen, X.L., Xu, B.H., Xue, J.M., Zhao, Y., Wei, C.C., Sun, J., Wang, Y., Zhang, X.D., and Geng, X.H. (2007), “Boron-doped zinc oxide thin films for large-area solar cells grown by metal organic chemical vapor deposition”, *Thin Solid Film.*, **515**, 3753-3756.
- Fah, C.P. and Wang, J. (2000), “Effect of high-energy mechanical activation on the microstructure and electrical properties of ZnO-based varistors”, *Solid State Ionics*, **132**, 107-109.
- Fan, J.C., Sreekanth, K.M., Xie, Z., Chang, S.L. and Rao, K.V. (2013), “Magnetism in band gap engineered sputtered $\text{Mg}_x\text{Zn}(1-x)\text{O}$ thin films”, *Prog. Mater. Sci.*, **58**, 847-985.
- Fujishima, A. and Honda, K. (1972), “Electrochemical photolysis of water at a semiconductor electrode”, *Nature*, **238**, 37-38.
- Gogurla, N., Sinha, A.K., Santra, S., Manna, S. and Ray, S.K. (2014), “Multifunctional Au-ZnO plasmonic nanostructures for enhanced UV photodetectors and room temperature NO sensing devices”, *Sci. Report.*, **4**, 6483-1-9.
- Golshahi, S., Rozati, R., Martins, S.M. and Fortunato, E. (2009), “P-type ZnO thin film deposited by spray pyrolysis technique: The effect of solution concentration”, *Thin Solid Film.*, **518**, 1149-1152.
- Hsu, Y.T., Lin, T.Y., Lan, W.H., Huang, Y.H., Chang, H.M., Wang, M.C., Yang, C.F. and Huang, K.F. (2014), “Photocatalytic study of bismuth doped Zinc Oxide prepared by spray pyrolysis: the effect of annealing”, *Optics*, **2014**, 1001-1013.
- Huang, Y.H., Lan, W.H., Shih, M.C., Lee, C.Y., Wang, Y.W. and Hsu, W.H. (2014), “The fabrication and stability study of bismuth doped zinc oxide prepared by spray pyrolysis”, ISNE 2014, Y13-11.
- Islam, M.R. and Podder, J. (2009), “Optical properties of ZnO nano fiber thin films grown by spray pyrolysis of zinc acetate precursor”, *Cryst. Res. Technol.*, **44**, 286-289.
- Kumar, N.S., Bangera, K.V., Anandan, C. and Shivakumar, G.K. (2013), “Properties of ZnO:Bi thin films prepared by spray pyrolysis technique”, *J. Alloy. Compound.*, **578**, 613-619.
- Lee, J.W., Subramaniam, N.G., Lee, J.C., Kumar, S.S. and Kang, T.W. (2011), “Study of stable p-type conductivity in bismuth-doped ZnO films grown by pulsed-laser deposition”, *Europh. Lett.*, **95**, 47002-1-6.
- Li, J.Z., Zhong, J.B., Zeng, J., Feng, F.M. and He, J.J. (2013), “Improved photocatalytic activity of dysprosium-doped Bi_2O_3 prepared by sol-gel method”, *Mater. Sci. Semicond. Proc.*, **16**, 379-384.
- Lin, M.S. and Chen, C.C. (2010), “Fabrication of the selective-growth ZnO nanorods with a hole-array pattern on a p-type GaN: Mg layer through a chemical bath deposition process”, *Thin Solid Film.*, **518**, 7398-7402.
- Lin, W. and Yan, X. (2011), “The comparison of ZnO nanowire detectors working under two wavelengths of ultraviolet”, *Solid State Commun.*, **151**, 1860-1863.
- Paraguay, F.D., Estrada, W.L., Acosta, D.R.N., Andrade, E. and Yoshida, M.M. (1999), “Growth, structure and optical characterization of high quality ZnO thin films obtained by spray pyrolysis”, *Thin Solid Film.*, **350**, 192-195.
- Pradhan, S., Karak, S. and Dhar, A. (2012), “Enhancing the performance of nanostructured zinc oxide/polymer-based hybrid solar cells using ammonia as a structural and interfacial modifier”, *J. Phys. D: Appl. Phys.*, **45**, 235104-1-8.
- Rastogi, A.C., Desu, S.B., Bhattacharya, P. and Katiyar, R.S. (2004), “Effect of strain gradation on luminescence and electronic properties of pulsed laser deposited zinc oxide thin films”, *J. Electroceram.*, **13**, 345-352.
- Senthilvelan, S., Chandraboss, L., Karthikeyan, B., Natanapatham, L. and Murugavelu, M. (2013), “ TiO_2 , ZnO and nanobimetallic silica catalyzed photodegradation of methyl green”, *Mater. Sci. Semicond. Proc.*, **16**, 185-192.
- Song, L., Chen, C. and Zhang, S. (2011), “Preparation and photocatalytic activity of visible light-sensitive selenium-doped bismuth sulfide. Powder Technology”, *Pow. Tech.*, **207**, 170-174.
- Szabo, T., Nemeth, J. and Dekany, I. (2004), “Optical properties of Indium-Doped ZnO nano-films prepared by spray pyrolysis and hydrothermal synthesis”, *Colloids Surf.*, **A230**, 23-35.
- Wan, S., Lu, W. and Liu, W. (2010), “Stress and electric displacement distribution near phase boundary in

- lead zirconate titanate”, *JPN J. Appl. Phys.*, **49**, 061102-1-5.
- Wongkalasina, P., Chavadej, S. and Sreethawonga, T. (2011), “Encapsulation of CdO/ZnO NPs in PU electrospun nanofibers as novel strategy for effective immobilization of the photocatalysts”, *Coll. Surf.*, **A384**, 519-528
- Wu, C.C., Wu, D.S., Lin, P.R., Chen, T.N. and Horng, R.H. (2009), “Repeated growing and annealing towards ZnO film by metal-organic CVD”, *Chem. Vapor Deposit.*, **15**, 234-236.
- Xu, C.X., Sun, X.W., Zhang, X.H., Ke, L. and Chua, S.J. (2004), “Photoluminescent properties of copper-doped zinc oxide nanowires”, *Nanotechnology*, **15**, 856-861.
- Yu, C.C., Hsu, Y.T., Lee, S.Y., Lan, W.H., Kuo, H.H., Shih, M.C., Feng, D.J.Y. and Huang, K.F. (2013), “Effects of doping ratio and thermal annealing on structural and electrical properties of boron-doped ZnO thin films by spray pyrolysis”, *JPN J. Appl. Phys.*, **52**, 065502-1-5.
- Zhong, J.B., Li, J.Z., Lu, Y., He, X.Y., Zeng, J., Hu, W. and Shen, Y.C. (2012), “Fabrication of Bi³⁺-doped ZnO with enhanced photocatalytic performance”, *Appl. Surf. Sci.*, **258**, 4929-4933.